View metadata, citation and similar papers at core.ac.uk
brought to you by CORE
provided by Elsevier - Publisher Connector

Available online at www.sciencedirect.com

Physics Procedia 1 (2008) 545–552

Physics Procedia

www.elsevier.com/locate/procedia

Proceedings of the Seventh International Conference on Charged Particle Optics

Dynamic blanking control of single column multi-electron-beam system

Osamu Kamimura[a,*], Hiroya Ohta[a], Sayaka Tanimoto[a], Makoto Sakakibara[a], Yoshinori Nakayama[a], Yasunari Sohda[a], Masato Muraki[b], Susumu Gotoh[b], Masaki Hosoda[b], Yasuhiro Someda[b], Kenji Tamamori[c], Futoshi Hirose[c], Kenichi Nagae[c], Kazuhiko Kato[c], Isamu Seto[d], Masamichi Kuwabara[d], Masahiko Okunuki[b]

[a]*Central Research Laboratory, Hitachi, Ltd., 1-280 Higashi-Koigakubo, Kokubunji, Tokyo 185-8601, Japan*
[b]*Nanotechnology & Advanced System Research Laboratory, Canon Inc., 23-10 Kiyohara-Kogyodanchi, Utsunomiya, Tochigi 321-3298, Japan*
[c]*Canon Research Center, Leading-Edge Technology Research Headquarters, Canon Inc., 30-2 Shimomaruko 3-choume, Ohta-ku, Tokyo 146-8501, Japan*
[d]*Utsunomiya Optical Products Operations, Canon Inc., 20-2 Kiyohara-Kogyodanchi, Utsunomiya, Tochigi 321-3292, Japan*

Received 9 July 2008; received in revised form 9 July 2008; accepted 9 July 2008

Abstract

Dynamic individual beam control in a multi-electron-beam system was demonstrated. In a multi-beam system, individual beam blanking and accurate correction of each beam position and irradiation dose are essential. In this paper, 16 beams in a 1024-beam system were individually blanked at 100-MHz frequency. Individual beam blanking was verified by pattern delineation. The beam position was corrected by the data shift through the feedback from the positions of formerly delineated patterns. The irradiation dose was corrected by measuring the dose of each beam and calibrating the irradiation time. Moreover, a movable blanking aperture was installed to improve the uniformity of blanking control. Finally, these corrections were evaluated by measuring the line widths in delineated patterns smaller than 65 nm. As a result, positioning accuracy within 1 pixel and dose deviation within 2.4% were achieved. In conclusion, it was clarified that our multi-beam-system has potential applications in semiconductor device manufacturing and inspection. © 2008 Elsevier B.V. Open access under CC BY-NC-ND license.

PACS: 41.85.-p; 85.40.-e; 85.40.Hp; 85.85.+j

Keywords: Multi-beam system; Single column; Electron beam; Inspection; Lithography; Micro-electro-mechanical system (MEMS) technology

1. Introduction

In the field of semiconductor device production, the miniaturization and concentration of circuit patterns and increases in wafer size have continued to progress. Accordingly, high-resolution and high-throughput equipment to inspect, measure, and manufacture these devices is strongly needed. One possible tool to meet these demands, is an

* Corresponding author. Tel.: +81-42-323-1111; fax: +81-42-327-7706
E-mail address: osamu.kamimura.ae@hitachi.com

doi:10.1016/j.phpro.2008.07.137

electron-beam system. However, although it can attain high resolution due to its short wavelength, the standard single electron beam cannot achieve both high resolution and high throughput because Coulomb interaction limits the resolution. Moreover, problems with the brightness limit of the electron gun also occur with a single beam. To achieve high resolution and high throughput without these problems, multi-electron-beam systems have been proposed.

Multi-electron-beam systems can be roughly divided into three types: 1) multi-column systems with multi-sources [1-3], 2) single-column systems with multi-sources [4-6], and 3) single-column systems with a single source [7-13]. We have developed a single-column system with a single source [7], namely a beam-split-array (BSA), and we demonstrated the proof-of-concept (POC) with 1024 multiple beams [13]. This system is simpler than the others and has a significant advantage in stability and in needing fewer calibrations.

In a multi-beam system, uniformity of optical property, individual beam blanking and accurate correction of each beam position and irradiation dose are essential. We have reported the verification of 1024 multi-beam construction as well as and the evaluation of projection optics, which had a beam size and distortion displacement of less than 60 nm even in off-axial beams [13]. In this paper, we demonstrate dynamic individual beam blanking, individual beam position calibration and individual dose control using pattern delineation. With these results we verify the potential of our multi-beam-system and realize the prospect of applying it in semiconductor device inspection or lithography.

2. System description and experimental setup

Fig. 1 illustrates a schematic diagram of our system called a beam-split-array (BSA). The beam is emitted from a single LaB_6 thermal-emission electron source with an acceleration voltage of 50 kV. It becomes parallel through the collimator lens and illuminates on the multi-source-module (MSM) [13, 14], which forms multiple beams. The MSM consists of three devices, an aperture array (AA), a static lens array (SLA), and a blanker array (BLA), which are fabricated using micro-electro-mechanical system (MEMS) technology. Images showing the appearance of the SLA and the BLA are in Fig. 2.

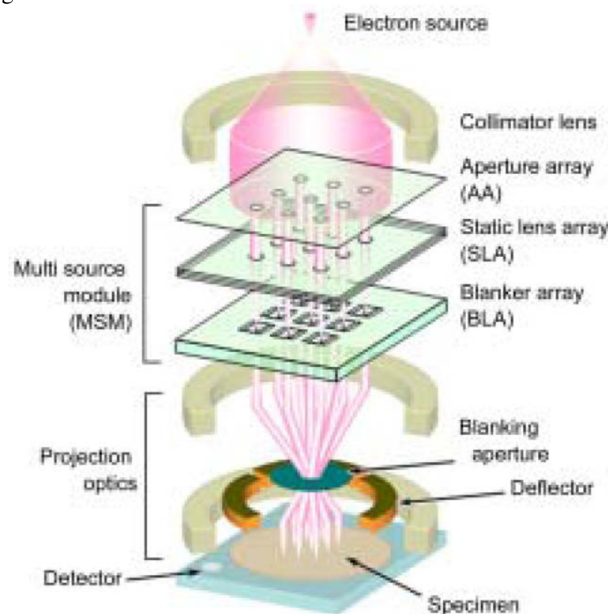

Fig. 1. Schematic diagram of multi-electron-beam system.

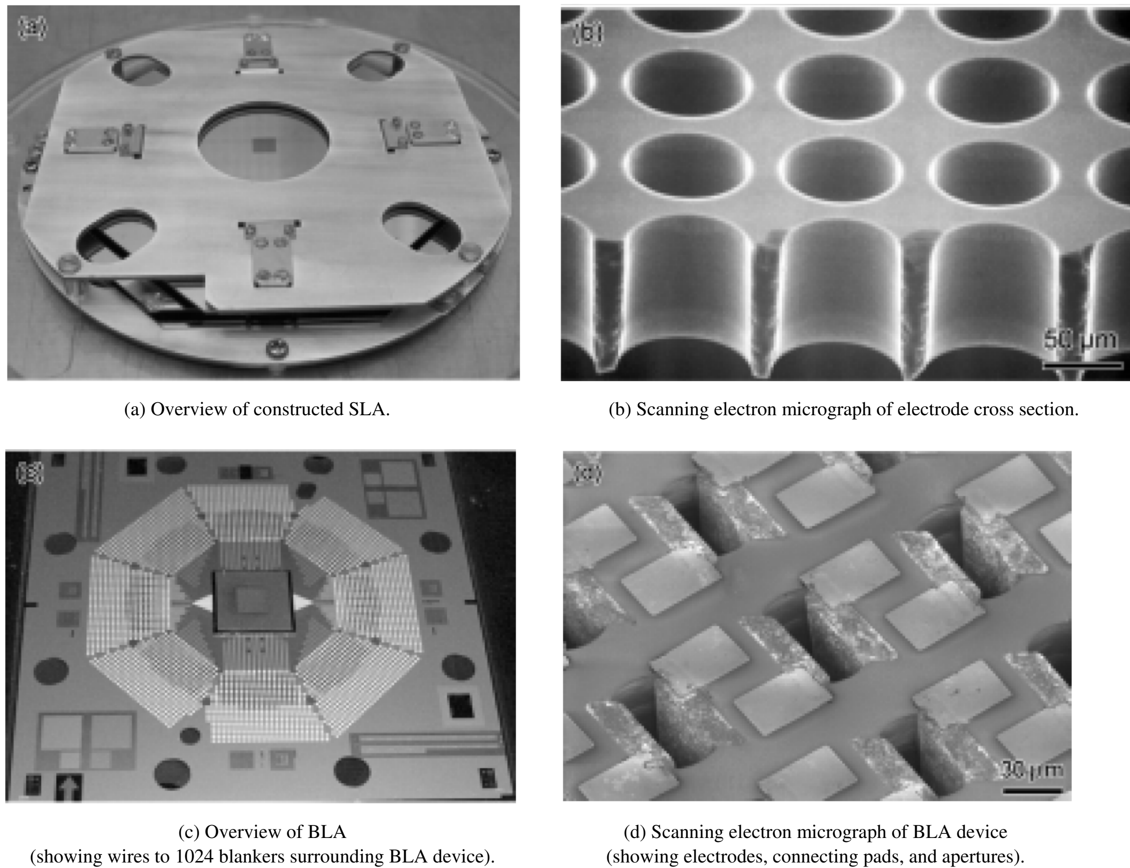

(a) Overview of constructed SLA.

(b) Scanning electron micrograph of electrode cross section.

(c) Overview of BLA
(showing wires to 1024 blankers surrounding BLA device).

(d) Scanning electron micrograph of BLA device
(showing electrodes, connecting pads, and apertures).

Fig. 2. Appearances of SLA and BLA.

The AA is a silicon aperture with 50-µm-diameter holes arranged in 102-µm spacing in a 32 × 32 two-dimensional square array. It divides the illuminated beam into 1024 multiple beams (to simplify the illustration, only nine beams are shown in Fig. 1).

The SLA is a three-electrode Einzel lens with 80-µm-diameter and 200-µm-deep holes for each divided beam (Fig. 2(a) and 2(b)). It focuses each divided beam to form intermediate images of the electron source at the position of the BLA. In our system, the SLA was constructed practically from the triple Einzel lens due to voltage application limits.

The BLA has pairs of electrodes as blankers for each focused beam (Fig. 2(d)). The gap between electrodes for each beam is about 25 µm and the length of each electrode is about 200 µm. At the BLA, a blanking voltage is applied individually for each beam and the deflected beam is cut off at the blanking aperture in the projection optics.

The intermediate source images at the BLA are demagnified through the projection optics. The projection optics is constructed from a double lens-doublet for a demagnification ratio of about 1/50, and includes the blanking aperture and deflector (in Fig. 1 only a single lens-doublet is depicted). The optical properties of the projection optics were evaluated, showing that beam size and distortion displacement were less than 60 nm even for off-axial beams [13].

The spacing of beams on the specimen is set to 2.048 μm. The beams, which pass the blanking aperture, are scanned together on the specimen by the deflector. The scan width of the deflector, which is set to be the same as the beam spacing, is divided into 128 × 128 pixels: thus, each pixel corresponds to a 16-nm square. It is possible to add some extra pixels when scanning by the deflector. If the number of irradiation pixels is kept at 128 × 128, the scan area of each beam stays at 2.048 μm. However, if we change the starting pixel number of one of the beams, the scan area of that beam will shift, but the others will not. This method can be used to calibrate the beam positional error due to distortion of the projection optics without an individual beam shifter, which we call a "data shift".

The beam irradiates each pixel intermittently like a pulse. The irradiation time for each beam on each pixel can be controlled by the off-blanking time of the BLA within 10 nsec (usually between 2 to 8 nsec) resulting in gray-scale-like variations. This irradiation assignment on a specimen with gray-scaled pixels is the same as a bitmap. If there is any deviation in beam current among the beams, the dose will be calibrated by optimizing the irradiation time, which we call a "dose control". The period of irradiation between pixels is 10 nsec, which means the irradiation frequency is 100 MHz.

The blanking aperture is located in the back focal plane (BFP) of the first projection lens. The position of the blanking aperture in the BFP effects both the optical property and irradiation dose. A movable blanking aperture is installed to improve both effects.

In our system the current of each beam was about 0.2 nA and to detect this weak beam we used a transmission method [13]. This detection system leads to higher contrast than a conventional reflection method.

Some patterns were delineated to verify the individual blanking control. In the delineation, chemically amplified negative- and positive-tone resists were used. The sensitivities were from 10 to 200 μC/cm^2, depending on the resist.

Fig. 3 is a photograph of our multi-beam system. This is based on the Hitachi HL-800D lithography system, and all lenses and the MSM were newly designed and installed.

Fig. 3. Experimental column of multi-electron-beam system.

3. Experimental results and discussions

Fig. 4 shows a result of the 1024-multi-beam formation, which also demonstrates a low distorted projection. Each beam has a square shape due to the window in the transmission method detector, even though each beam is actually spot-shaped.

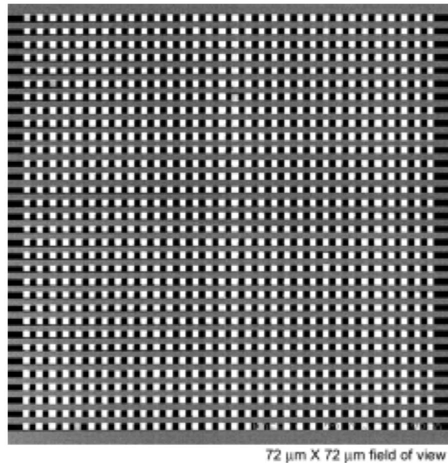

Fig. 4. 1024 beams formation.

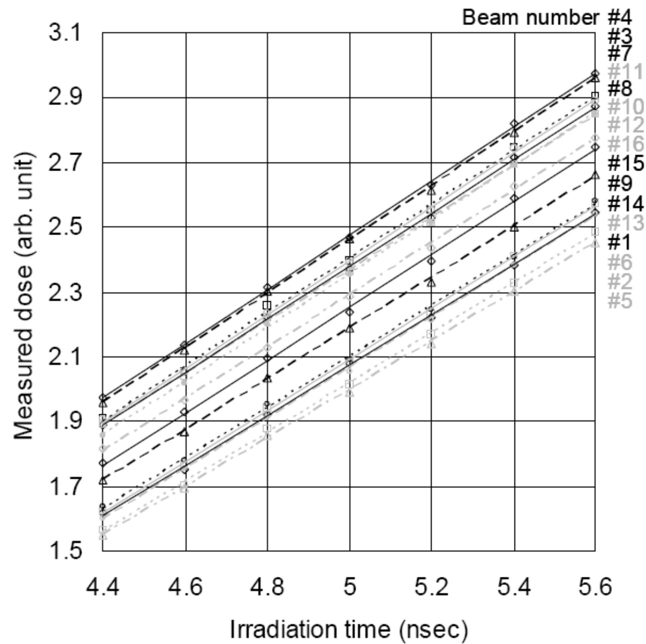

Fig. 5. Dose-to-irradiation time measurement.

We can control any 16 beams in these 1024 multiple beams, and 4 × 4 near optical axial beams were selected to demonstrate the individual blanking control.

To blank each beam, blanking voltage of 7 V is applied through wiring from the blanking driver (Hitachi High-Tech D E Technology Co., Ltd.) to the blanker electrodes at the BLA. The translation was verified and the crosstalk between wires was confirmed to be less than our measurement limit even at the frequency of 100 MHz. Fig. 5 shows irradiated dose measurement per irradiation time for each beam for 16 near-axial beams. The dependence on irradiation time is approximately fitted linear, which shows that beams are controlled and the measurement is successful at 100-MHz frequency. However, there are differences in height and inclination among the lines, which indicates difference in the dose, as will be discussed later.

To verify dynamic individual beam blanking control and bitmap data assignment, some resist patterns were delineated on silicon wafers. Fig. 6 shows one of the results of individual beam blanking at 100 MHz. This pattern is constructed of 16 simultaneously delineated individual patterns of 1:1 lines and spaces with 130-nm pitch (the dotted lines in the figure indicate boundaries between beams). Fig. 7 shows a cross section of the pattern, which is almost the same as in Fig. 6 but is delineated on a positive-tone resist. The rectangular-shaped cross sections of lines verify the performance of this system. Fig. 8 shows another result. This pattern consists of 65-nm wide lines with 5-degrees pitch and circles, which is divided into 16 individual patterns with dotted lines indicating beam boundaries. As can be found in Figs. 6, 7 and 8, our system with bitmap data is effective with any pattern delineation.

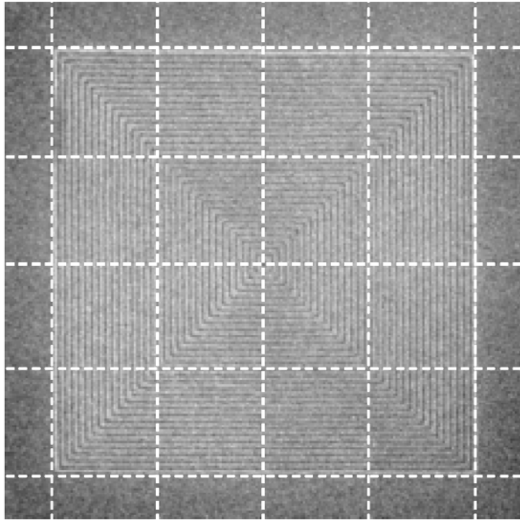

Fig. 6. 16 individual pattern delineation with 65-nm lines and spaces.

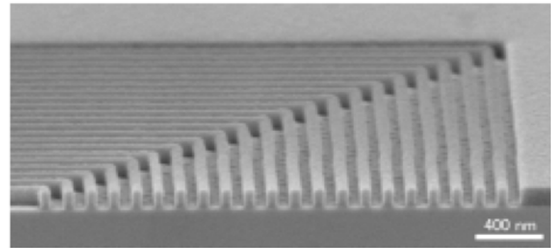

Fig. 7. Cross section of 65-nm lines and spaces.

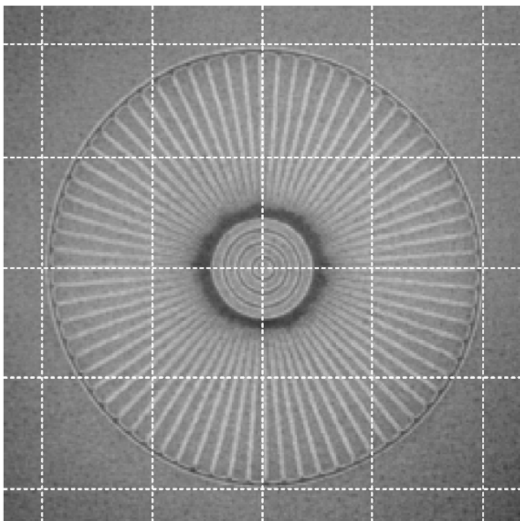
Fig. 8. Angled lines and circles pattern.

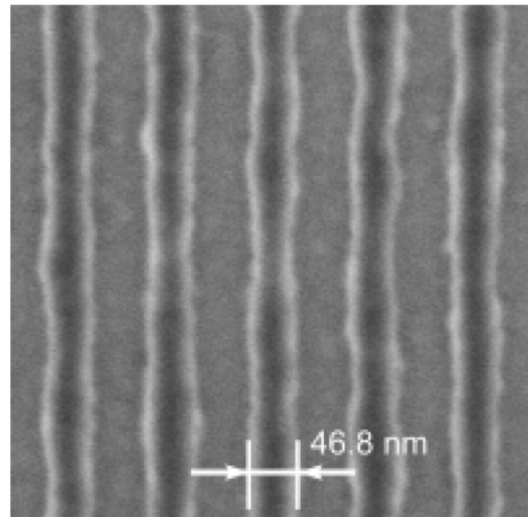

Fig. 9. Delineated lines and spaces pattern with 46.8 nm line width.

Fig. 9 shows lines and spaces pattern with measured line width of 46.8 nm. At present, to verify minimum-line-width delineation, we need to improve a resist process.

Fig. 10 is the pattern delineation result with the formerly constructed MSM as a demonstration of the data shift. In Fig. 10(a), the pattern of the lower right beam was shifted. A gap of pattern due to the shift is indicated by an arrow. This pattern shift was caused by a positional error of the beam resulting from some substances being in this MSM accidentally. The data shift was verified by measuring the deviation of the resist pattern in Fig. 10(a) and adjusting it in the next delineation. As shown in Fig. 10(b), the shifted pattern was calibrated. Using the data shift, positional accuracy was maintained within one pixel. In this experiment, we used the results of the previous delineation to adjust the beam position, but it can be calibrated in less time by measuring beam positions accurately.

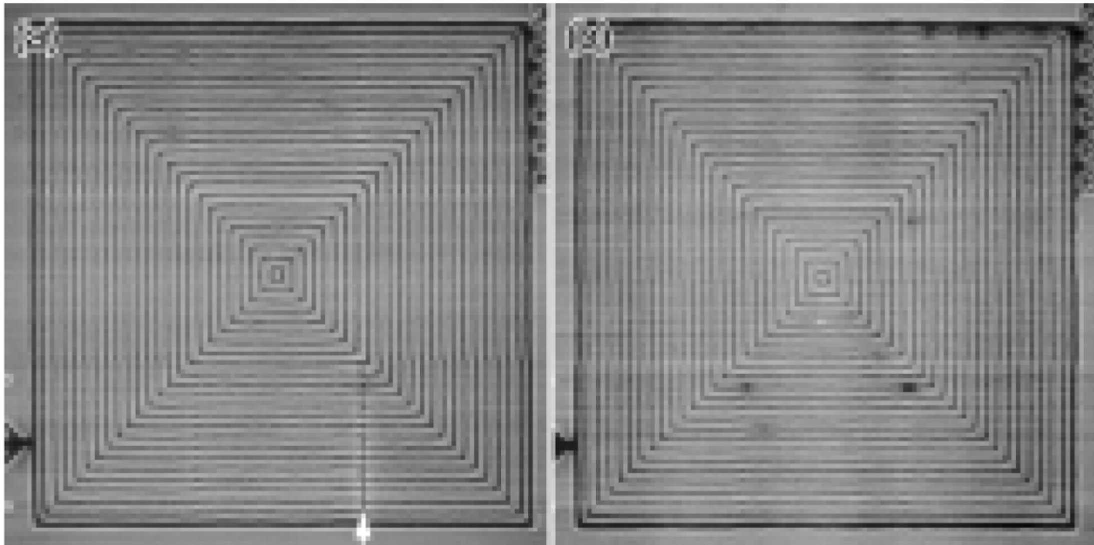

Fig. 10. Verification of data shift with 65-nm lines and spaces.

Irradiation doses of 16 beams were calibrated by measuring the irradiation-time dependence of the dose and assigning a suitable irradiation time to each beam. As shown in Fig. 5, there was some deviation in the irradiation dose among the 16 beams. The irradiation time of each beam was set depending on the inclination (meaning the dynamic current of each beam) to calibrate the dose. The results of calibration showed that the difference in doses among the beams was improved from 21% to 2.4%. In addition, patterns the same as in Fig. 6 were delineated before and after dose calibration, because a delineated pattern is sensitive to irradiation dose. As a result, the deviations of line width were improved from 19% to 8% with a measurement error of about 5% due to line edge roughness.

We verified the fundamental properties of the multi-beam system: individual beam blanking, calibration of beam position and irradiation dose. These results lead a prospect that our multi-beam system has enormous potential for application to semiconductor device manufacturing and inspection.

4. Summary

To verify the dynamic individual beam control, individual pattern delineation, calibration of beam position by date shift, and dose calibration were executed. Simultaneous delineation of 16 individual patterns meant that we were able to verify individual beam blanking control at 100-MHz frequency. Delineated patterns in several shapes, including angled lines and circles, were shown in this paper, although any shapes are possible. Additionally, methods to calibrate beam positions and to supply a uniform irradiation dose were established. The calibration of beam position was executed by a data shift and the deviation of delineated patterns was maintained within 1 pixel. The irradiation doses were normalized by dose control at 2.4%. Moreover, by calibrating the irradiation dose, the delineated patterns also normalized their line width within 8% of the averaged value. With these results, we verified the concept of our single-column multi-electron-beam system, which has potential applications in inspection or lithography processes of semiconductor device products. It is necessary to optimize the controllable beam number, optical property, and measurement accuracy that are suitable for each application.

Acknowledgements

We would like to thank Mr. T. Kanosue at Hitachi High-Tech Fielding Corporation and Dr. N. Saito, Dr. H. Yoda and Mr. K. Ando at Hitachi High-Technologies Corporation for their technical and theoretical support. We extend our gratitude to Mr. H. Yoshinari, Mr. T. Yagi and Mr. H. Ono at Canon Inc. for their valuable technical advice and support. Part of this work was supported by the New Energy and Industrial Technology Development Organization (NEDO).

References

[1] L.P. Muray et al., J. Vac. Sci. Technol. B 18 (2000) 3099.
[2] T.R. Groves and R.A. Kendall, J. Vac. Sci. Technol. B 16 (1998) 3168.
[3] T. Haraguchi et al., J. Vac. Sci. Technol. B 22 (2004) 985.
[4] E. Yin et al., J. Vac. Sci. Technol. B 18 (2000) 3126.
[5] S.T. Coyle et al., J. Vac. Sci. Technol. B 22 (2004) 501.
[6] S. Tanimoto et al., Jpn. J. Appl. Phys. 42 (2003) 6672.
[7] M. Muraki and S. Gotoh, J. Vac. Sci. Technol. B 18 (2000) 3061.
[8] H. Yasuda et al., J. Vac. Sci. Technol. B 14 (1996) 3813.
[9] G. Winograd et al., J. Vac. Sci. Technol. B 18 (2000) 3052.
[10 P. Kruit and M.J. Wieland, MNC 2004 abstracts, p. 310.
[11] http://www.PML2.com/
[12] N. Nakasuji et al., Jpn. J. Appl. Phys. 44 (2005) 5570.
[13] O. Kamimura et al., J. Vac. Sci. Technol. B 25 (2007) 140.
[14] S. Tanimoto et al., J. Vac. Sci. Technol. B 25 (2007) 380.